applied sciences

MDPI

Article

The Effect of Electrolytes and Urea on the Ethyl Lauroyl Arginate and Cellulose Nanocrystals Foam Stability

Agnieszka Czakaj *, Marcel Krzan and Piotr Warszyński

Jerzy Haber Institute of Catalysis and Surface Chemistry, Polish Academy of Sciences, ul. Niezapominajek 8, 30-239 Krakow, Poland; marcel.krzan@ikifp.edu.pl (M.K.); piotr.warszynski@ikifp.edu.pl (P.W.)
* Correspondence: agnieszka.czakaj@ikifp.edu.pl

Abstract: Carboxylated cellulose nanocrystals (cCNC) are highly dispersible particles useful in many industries. In particular, they can be applied to form Pickering emulsions and foams for "green" applications in the cosmetics, pharmaceutical industry or food processing. We demonstrated that carboxylated cellulose nanocrystals enhance foamability and foam stability when mixed with cationic surfactant ethyl lauroyl arginate (LAE), having superior properties over sulfated cellulose nanocrystals (sCNC) concerning surfactant concentration range and foam volume. Mixtures of LAE and cCNC were characterized for their hydrodynamic diameter, zeta potential, surface tension and surface rheological properties. The influence of electrolytes, namely, sodium chloride, guanidine hydrochloride and sodium salicylate, and the addition of concentrated urea to LAE-cCNC mixtures on foamability and foam stability were investigated. Electrolytes in the concentration of 5 mM showed a moderate effect on foam stability. In contrast, spectacular foam collapse was detected after adding concentrated urea. The preliminary rheological data from the pendant drop oscillations revealed low elastic modulus upon urea addition and the loss modulus that increased with the frequency, which suggested a viscous interfacial layer.

Keywords: ethyl lauroyl arginate; surface dilational elasticity; foam; interfacial rheology; cellulose nanocrystals

Citation: Czakaj, A.; Krzan, M.; Warszyński, P. The Effect of Electrolytes and Urea on the Ethyl Lauroyl Arginate and Cellulose Nanocrystals Foam Stability. *Appl. Sci.* **2022**, *12*, 2797. https://doi.org/10.3390/app12062797

Academic Editor: Fabrice Goubard

Received: 2 February 2022
Accepted: 4 March 2022
Published: 9 March 2022

1. Introduction

Cellulose present in plant cell walls is the most abundant polysaccharide and sustainable biopolymer on the Earth. It consists of glucose molecules linked with β-1,4-glycosidic bonds. As a raw material, cellulose has been used in the industry for 150 years [1]. Nanocellulose particles, with at least one dimension in the nanoscale, have been increasingly applied in the newest technologies [2,3]: piezoelectricity and wearable electronics [4], pigments [5], flocculants [6], wound healing materials, drug carriers, implants and tissue engineering [7], coatings, adhesives, antibacterial packaging materials [8], thickeners and rheology modifiers [9], nano-templates, [10] reinforcing agent for composites, foams and aerogels [11], Pickering foams and emulsions [12].

Cellulose nanocrystals released by chemical hydrolysis or oxidation were first produced in 1947. They possess three essential properties: colloidal stability in polar solvents, nano-size and high crystallinity. Since 1990, they have been manufactured in tonne-per-day quantities. They are suitable for commercial applications, including the preparation of foams. In the process of sulfuric acid hydrolysis, glycosidic bonds of cellulose chains are broken, especially in less crystalline regions, and some hydroxy groups on cellulose surfaces are esterified. Released nano-sized crystalline particles, partially esterified, are called sulfated cellulose nanocrystals (sCNC) (containing carbon–oxygen–sulfur bond) [13].

Carboxylated cellulose nanocrystals (cCNC) can be produced in a batch process with dilute hydrogen peroxide oxidation [14]. The cCNC has a relatively low surface charge density compared to sulfated cellulose nanocrystals. They are also less crystalline and have a relatively high surface area.

Cellulose is chiral in many length scales from molecules up to mesophases. Importantly, nanocellulose crystals and fibers are twisted [15], which affects the exposure of their more hydrophobic crystallographic planes at the air/water interface. Depending on their concentration, cellulose nanocrystals may form liquid crystals in water [16]. The liquid crystalline behavior of cellulose nanocrystals (CNC) is solvent-dependent, which can be explained with more efficient hydrogen bonding between CNC at lower dielectric screening. Cellulose nanocrystals form needle-like elongated micro-aggregates with broad size distribution in low dielectric solvents [17].

Ethyl lauroyl arginate is a cationic surfactant manufactured from biodegradable compounds. It hydrolyses to other surface-active substances in water: Nα-lauroyl–L-arginine (LAS) or dodecanoic (lauric) acid. In our previous work, we described its interfacial properties [18] and determined critical micelle concentration (CMC) at about 1 mmol/L.

Foaming properties are interesting from many technological perspectives, including flotation and detergency. There are several methods of foam formation characterization, including the double syringe technique [19], which provides foams consisting of tiny bubbles of relatively uniform size [20]. Foaming experiments carried out with the double syringe for a commercial brand of LAE (85% purity) showed that at concentrations below 0.35 mM, its solution did not form foams surviving more than several minutes. On the contrary, when mixed with hydrophilic sulfated cellulose nanocrystals, foams could be stable for up to 4 h [21]. Nanometric sCNC with sulfate hydrophilic groups moderately interact with LAE at low surfactant concentrations, and particle zeta potential and hydrodynamic diameter do not change significantly. The explanation of enhanced foam stability in LAE-sCNC mixtures is far from trivial. A slight increase in dispersion viscosity, high interfacial shear elasticity and flow-induced plugs in the Plateau borders may contribute to the enhanced foam stability. On the other hand, sCNC aggregates in the foam films may have an opposite antifoaming effect.

Upon aggregation, cellulose nanocrystals form rods with a high aspect ratio and rectangular cross-section that can be crucial for explaining foam stability in the mixtures with surfactants. The aspect ratio of nanocellulose can be a key parameter determining the stability of Pickering emulsions [22]. Emulsion stability is also inversely proportional to the surface charge density of cellulose nanocrystals, since less charged CNC are more amphiphilic [23]. Thus, cellulose nanocrystals' surface charge density can affect interfacial properties and foaming properties at the liquid/air interface [24].

The redispersion of sulfated CNC can impact the rheological properties of their dispersions [25]. They adsorb at the liquid/air interface after several hours when the addition of salt screens their charge [26]. CNC forms lyotropic liquid crystals at concentrations above 1% by weight [27]. It was shown that the addition of cellulose nanocrystals enhances the stability of methylcellulose foams after the formation of gels [28]. There were other reports concerning the influence of nanocellulose on foaming properties [29], where size and bulk rheology of nanocellulose played a significant role. However, only a few studies have been related to simple liquid foams without gelled phase, without polymers as additives and with nanocellulose in the form of nanocrystals.

Various additives modify the electrostatic properties of nanoparticles, the interaction of nanoparticles and surfactants and the foaming properties of their mixtures. The addition of monovalent electrolyte decreases electrostatic repulsion between particles and enhances surfactant adsorption at the interface, due to lower electrostatic repulsion between ionic molecules [30]. Sodium salicylate belongs to organic counterions and hydrotropes solubilizing hydrophobic compounds. It can interact with other surfactants or nanoparticles electrostatically and hydrophobically. It enables the transition of surfactant structure in the solution from spherical micelles to worm-like micelles [31]. Research on interfacial layer viscoelasticity in such systems is rarely reported for surfactant–nanoparticle systems. Some works were devoted to protein interfacial layers that demonstrated that sodium salicylate could dramatically reduce interfacial viscoelasticity of the protein films and change the

properties of wheat dough. It was hypothesized that sodium salicylate acts as a hydrogen bond breaker [32,33].

As it is known from the literature, urea increases critical micelle concentration of surfactants [34], increases counterion dissociation [35], displaces the water from the surface of ionic surfactants, helps solvate the hydrophobic micelle cores by localizing at their surfaces, and changes the micelle shape and the number of surfactants associating in the micelle [36]. Recent data show urea orients at the interface within the hydrogen-bonded water network. Its orientation depends on the sign of the charged interface—the net orientation of urea is possible only in the presence of surfactants. Depending on the concentration, urea orients with its C=O group toward a positively charged interface, as shown by characteristic vibrational modes of urea detected by SFG spectroscopy [37].

It was evidenced that urea can improve the solubility and stability of cellulose in alkaline solutions [38]. Urea can compete with water for hydrogen bonding that, together with ionic interactions, contribute the most to the protein tertiary structure. The structure might be entirely destroyed at the urea concentration of 8 mol/L. Guanidine hydrochloride (GuaHCl), is an even stronger protein denaturant than urea. It contains a common cation as a positively charged group of LAE and is well known for its chaotropic properties. In protein solutions, it acts as an unfolding agent [39]. It is also known that urea forms hydrogen bonding with protein backbone amides at high concentrations, while guanidine hydrochloride acts preferentially on hydrophobic residues of the protein [39]. Ethyl lauroyl arginate contains an amide bond between the hydrocarbon chain and guanidinium hydrophilic headgroup; therefore, it can be hypothesized that urea should have a strong effect on LAE interfacial layer. The additional factor that should be taken into account while comparing the urea and GuaHCl effect is the low concentration of GuaHCl that can be used in the experiment to avoid aggregation of surfactant and particles.

In this work, we compared the foaming properties of mixtures of LAE and carboxylated and sulfated CNC. Then, we studied the effect of the addition of electrolytes, a common salt—NaCl, hydrotropic sodium salicylate, and chaotropic guanidine hydrochloride or urea on ethyl lauroyl arginate—carboxylated CNC dispersions bulk and interfacial properties. We attempted to correlate surface tension and dilational viscoelastic properties of dispersions with their foamability and foam stability. Since LAE is a food-grade cationic surfactant with antimicrobial activity against a wide range of food pathogens and spoilage organisms, its foaming properties, enhanced with biopolymeric nanoparticles, can find potential application in cosmetic or pharmaceutical products. Our findings could contribute to the reduction in the amount of surfactant that is necessary to show significant surface activity, emulsification and foaming properties. On the other hand, they can provide information about the selection of components that could be used as defoamers.

2. Materials and Methods

Ethyl lauroyl arginate (LAE), under commercial name Mirenat-P/100 (about 90% LAE surfactant content), was generously provided by Vedeqsa (Barcelona, Spain). Sodium chloride (99%), guanidine hydrochloride (>99% purity), sodium salicylate and urea 8 M Bio Ultra was acquired from Sigma-Aldrich (Poznań, Poland). NaCl was calcinated at 650 °C for eight hours before use. The stock solution was prepared in deionized cold water (4 °C, ~20 MΩ cm) and then diluted to the appropriate concentration. Stock solution and dilutions were used within one day.

Commercially available carboxylated cellulose nanocrystals, DextraCel manufactured by Anomera (Montreal, QC, Canada), used in this work were in the form of sodium salt spray-dried powder with the specification: zeta potential range −40 to −50 mV, diameter 5–10 nm, length 150–200 nm, carboxyl content 0.12–0.20 mmol/g. As has been described by Delepierre et al. [40], cCNC are 150 ± 30 nm in length, 5 ± 2 nm in diameter (approx. round cross-section) with apparent hydrodynamic size 81 ± 1 nm. Their total charge measured by conductometric titration is 141 ± 10 mmol/kg, and surface charge density is 0.16 e/nm^2. The shear viscosity of 2% solution at 10 s^{-1} is 1.6 mPa s and is purely

Newtonian at 0.1–10 s^{-1}. Zeta potential is -21 ± 1 mV. Cellulose nanocrystals were dispersed carefully in water by adding small portions of CNC and stirring to achieve a concentration of 0.6% by weight. They were sonicated [Sonic 6D; Polsonic, Warsaw, Poland] after mixing. The cCNC dispersion was added drop by drop to surfactant solution under constant stirring. The concentration of 5 mM was chosen for electrolytes when preparing different mixtures of 0.3% by weight of cCNC from the same stock of particles 0.6 wt.%, dispersed in water to avoid particle aggregation, which may affect foaming properties and interfacial rheology.

2.1. Foaming

Foaming experiments were carried out with the double syringe technique [19–21]—with two single-use medical syringes of 60 mL volume connected by a narrow tube. First, 20 mL of LAE-CNC solution and 40 mL of air were mixed, and the solution passed from one syringe to the other ten times. After that, it stood vertically, and after about 15–30 s, it was possible to read out the foam and liquid levels and determine initial foam volume. Note that here, foam volume was measured only up to 280 min.

2.2. Particle Characterization

The size and zeta potential of cCNC nanoparticles and LAE-cCNC dispersions was measured, respectively, by dynamic light scattering [41] and by laser Doppler velocimetry with Malvern Nano ZS instrument as described earlier [21]. Each measurement was repeated three times. No viscosity correction was applied. The average error (standard deviation) of zeta potential measurement was 5 mV maximum.

2.3. Surface Tension

The surface tension of samples was measured using the pendant drop technique [42] with a Sinterface PAT-1M tensiometer immediately after surfactant solution or dispersion preparation. A drop of solution (11 µL) was created from a 2 mm diameter steel capillary and kept in the thermostated chamber for 2000 s. The camera recorded the drop profile, and the Young–Laplace equation was fitted to calculate the surface tension [43]. Drop oscillations were applied after reaching the surface tension equilibrium by imposing drop volume (area) changes of less than 10% of the volume. Then, Fourier transform of the surface tension variations was calculated and the surface dilational modulus was determined as the complex number [44]:

$$\varepsilon = A_0 \frac{\Delta\sigma_1}{\Delta A_1} = \varepsilon_r + i\varepsilon_i = \varepsilon_d + i\omega\nu_d \quad (1)$$

where $\varepsilon_r, \varepsilon_i$ are the real and imaginary part of the dilational elasticity modulus, ε_d is dilational elasticity, ν_d is the dilational viscosity, ω is the oscillation frequency, A_0 is the average area of the drop, ΔA_1 and $\Delta\sigma_1$ are the principal Fourier components of the area and surface tension variations that correspond to the frequency of drop oscillations.

3. Results and Discussion

3.1. Foaming

Figure 1 illustrates foam half-life (the time after which 50% of the foam breaks) as the function of surfactant concentration for foams generated after 10th cycle of mixing the air and the 20 mL of LAE-CNC dispersion in connected syringes.

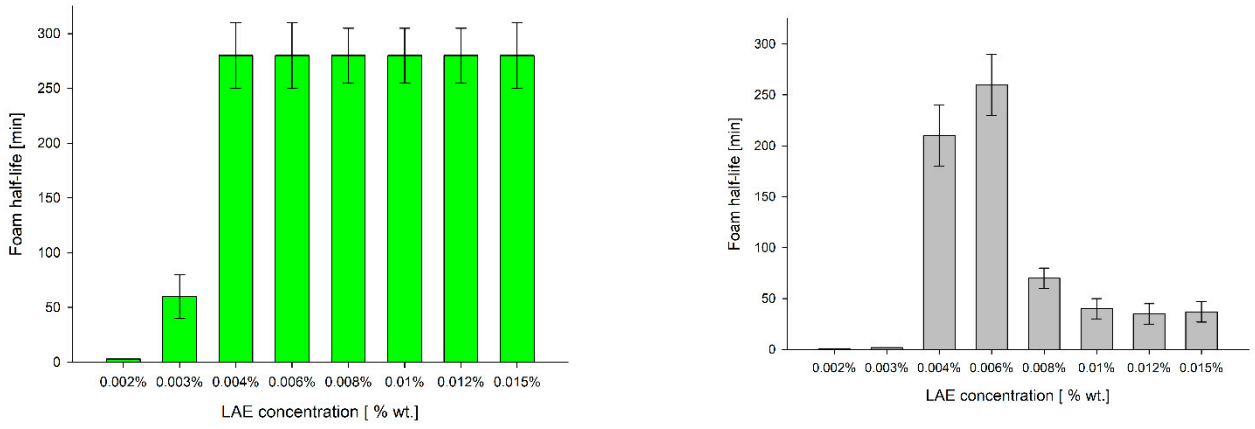

Figure 1. Foam half-life of dispersion of the 0.3 wt.% cellulose nanocrystals with various LAE concentrations; (**a**) cCNC; (**b**) sCNC, (see ref. [21]). Maximum observation time 280 min.

Foam and liquid volume could be measured after approximately 30 s and observed for up to 280 min. As shown in Figure 1a, for all concentrations above 0.004%, foam half-life was at least 280 min. In contrast, for sCNC foam half-life was at maximum for 0.006 wt.% of LAE and then decreased for higher surfactant concentrations (Figure 1b) [21]. The aggregation can be the reason for the limited foam stability in the case of sCNC. The results presented in Figure 1 show a threshold value of surfactant concentration (0.003%, 0.07 mM) in the LAE-cCNC mixture, at which foam stability significantly increased. That threshold value was slightly higher for sCNC (0.004 wt.%). Since the zeta potential of nanoparticles in the LAE-cCNC dispersion (−35 mV) was lower than in LAE-sCNC (−40 mV), they can be more amphiphilic, as suggested in [23].

The LAE concentration above the foam stability threshold (0.006 wt.%) was selected to study the effect of various additives on foaming and interfacial properties of the LAE-cCNC suspension. It should be noted that no stable foam can be formed at that surfactant concentration without nanoparticles. The results collected in Table 1 illustrate that at the surfactant concentration corresponding to the LAE-sCNC maximum foam lifetime, cCNC are much more efficient at foaming. The foam volume was almost doubled for carboxylated CNC compared to sulfated ones, while its stability was also prolonged.

Table 1. Initial foam volume and foam half-life in LAE 0.006 wt.%—CNC 0.3 wt.% dispersions with respect to CNC hydrophilic groups.

	LAE-sCNC	**LAE-cCNC**
Foam volume [mL]	19 ± 1	37 ± 1
Foam half-life [min]	260 ± 20	>280

To elucidate the possible reason for the differences in foam stability between two types of CNC for LAE concentration above 0.008 wt.%, we measured the dependence of cCNC hydrodynamic size on the surfactant concentration. The results are listed in Table 2. They show that carboxylated cellulose nanocrystals are resistant to aggregation up to 0.02 wt.% LAE. Moreover, they indicate that cCNC were less aggregated than sCNC. For the surfactant concentration 0.015 wt.% the hydrodynamic size of cCNC was 112 nm (PDI 0.44), significantly smaller and less polydisperse than for sCNC—187 nm (PDI 0.82) [21]. That seems to support the hypothesis that the defoaming effect of large aggregates can cause lower foam stability of sCNC-LAE dispersion.

Table 2. The hydrodynamic diameters of cCNC dispersions with increasing LAE concentrations.

cCNC 0.3 wt.% with	Hydrodynamic Diameter [nm] (Polydispersity Index)
0.008% LAE	87 (0.38)
0.01% LAE	88 (0.30)
0.015% LAE	112 (0.44)
0.02% LAE	206 (0.78)
0.05% LAE	~7000 (1.00)

Figure 2 illustrates the effect of additives—ionic and non-ionic—on the initial foam volume, generated with the double syringe technique. The addition of monovalent electrolytes, sodium chloride or guanidinium hydrochloride at a concentration of 5 mmol/L to LAE-cCNC mixtures did not the change foam volume significantly. The difference was seen for 5 mM sodium salicylate, which contains a bulky surface-active anion that can effectively penetrate the interfacial layer formed by cationic LAE and cCNC. The foam volume decreased to about 12 mL, more than three times with respect to LAE-cCNC without additives, or more than two times with respect to one with NaCl. The most significant effect of reducing the initial foam volume was seen for dispersions containing 6 mol/L urea. Right after the foam formation, it filled the whole syringe; however, it collapsed very quickly. The first possible readout of the foam and liquid volume characterizing the foamability, which could be compared with other systems, was made after 30 s.

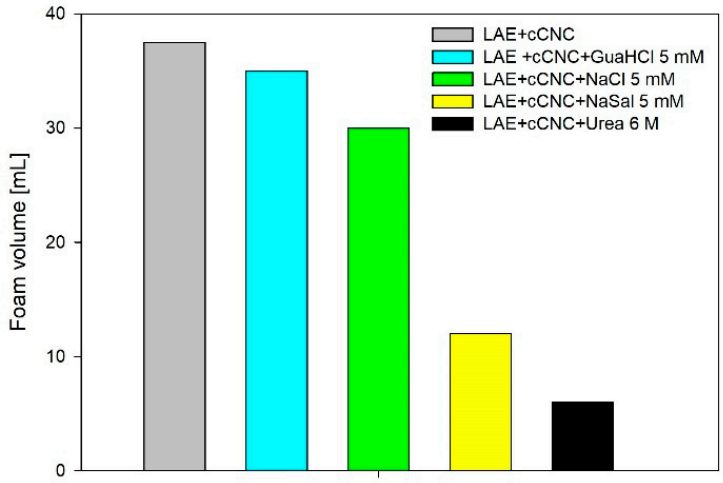

Figure 2. Foam volume of LAE 0.006 wt.% and carboxylated nanocrystals 0.3 wt.% with additional compounds in the dispersion.

Foam half-life for the LAE-cCNC dispersion with added electrolytes (NaCl, NaSal and GuaHCl) was reduced to c.a. 200 min (Figure 3). Note that the foam half-life of the dispersion with 5 mM of NaSal was the same as for other electrolytes, despite lower foamability. That means that the foam drainage rate was independent of the type of salt. As mentioned above, the most significant difference in foam stability was noted in the dispersion containing 6 mol/L urea. The foam half-life was reduced to less than 1 min, coinciding with the fast draining period.

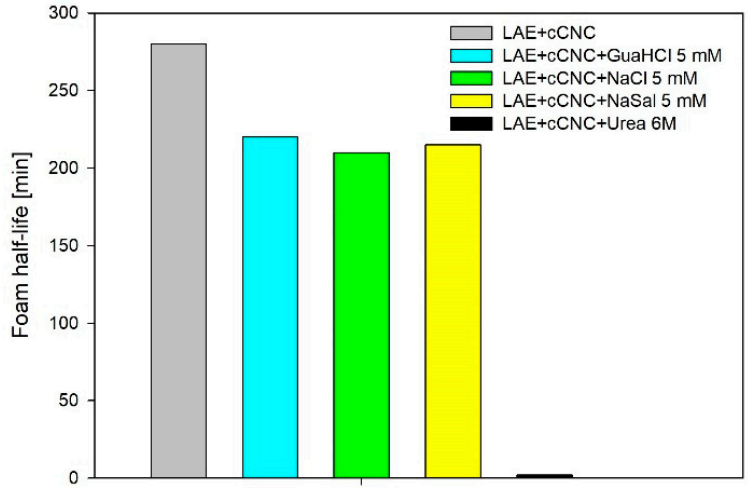

Figure 3. Foam half-life in the dispersion of LAE 0.006 wt.% and cCNC 0.3 wt.% with the addition of NaCl, NaSal, GuaHCl and urea.

3.2. Zeta Potential and Hydrodynamic Diameter

The results of the zeta potential and hydrodynamic diameter measurements of carboxylated CNC are collected in Table 3. Zeta potential measurements indicate that carboxylated nanoparticles are slightly less charged than sulfated [17]. Spray-dried powdered carboxylated CNC were easier to disperse upon sonication; however, the measured hydrodynamic diameter had large polydispersity. Upon adding 5 mM of NaCl or NaSal to LAE 0.006 wt.%—cCNC 0.3 wt.%, dispersion, the zeta potential was only slightly reduced, whereas the addition of the same concentration of GuaHCl decreased the potential by c.a. 10 mV. A similar decrease could be observed at the addition of 6 M of urea. In the case of NaCl and GuaHCl, the decrease in zeta potential was accompanied by a large (almost twice) increase in hydrodynamic diameter, indicating aggregation. No changes were observed when 5 mM NaSal was added to the dispersion, whereas for 6 mol/L urea, the dispersion turbidity almost disappeared, as seen by the naked eye. Nevertheless, the hydrodynamic diameter of 100 nm, with a considerably lower polydispersity, could be measured. The effect of urea was also checked for 0.015 wt.% LAE concentration. Similarly to 0.006 wt.% of LAE, the urea addition increased the dispersion size from 112 nm to 132 nm but reduced polydispersity from 0.44 to 0.35. The plausible explanation of those changes could be that despite the average size (by intensity) of the dispersion grows, the larger cellulose nanocrystals aggregates are destroyed by the addition of urea since it enhances cellulose solubility [38].

Table 3. Zeta potential and hydrodynamic diameter of cCNC dispersions of LAE 0.006% and additional compounds.

LAE 0.006 wt.%—cCNC 0.3 wt.% with:	Zeta Potential [mV]	Hydrodynamic Diameter [nm] (Polydispersity Index)
No additives	−35 ± 5	77 (0.44)
NaCl 5 mmol/L	−30 ± 5	197 (0.53)
Urea 6 mol/L	−26 ± 4	101 (0.28)
Sodium salicylate 5 mmol/L	−31 ± 4	108 (0.43)
Guanidine hydrochloride chloride 5 mmol/L	−26 ± 3	209 (0.52)

3.3. Surface Tension

Figure 4 illustrates surface tension kinetics in LAE-cCNC mixtures at LAE concentration 0.006 wt.% and cCNC 0.3 wt.%, in the presence of added 5 mM NaCl, NaSal, GuaHCl and 6 mol/L urea. In general, the addition of cCNC to the surfactant solution decreased the equilibrium surface tension from 48 mN/m for pure 0.006 wt.% LAE (cf. Figure 5) to 40 mN/m for the dispersion with 0.3 wt.% cCNC. Similar results were obtained previously for sCNC [21]. In the case of sodium chloride and guanidinium chloride addition, compared with "no salt" conditions, some decrease in the surface tension was observed at short adsorption times. That effect is similar to one observed for ionic surfactants resulting from the screening of the electrostatic interactions. On the other hand, at longer adsorption times, a small surface tension increase could be noted, which may be explained by aggregation of nanoparticles and more extensive surfactant binding to those aggregates in the suspension. That can be correlated with some reduction in foam stability.

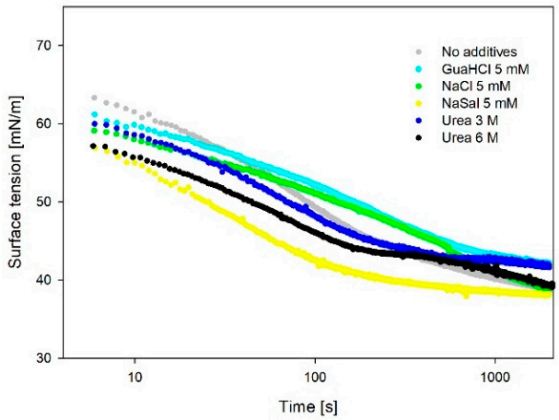

Figure 4. Surface tension of the dispersion of LAE 0.006 wt.% and cCNC 0.3 wt.% with the addition of NaCl, NaSal, GuaHCl and urea.

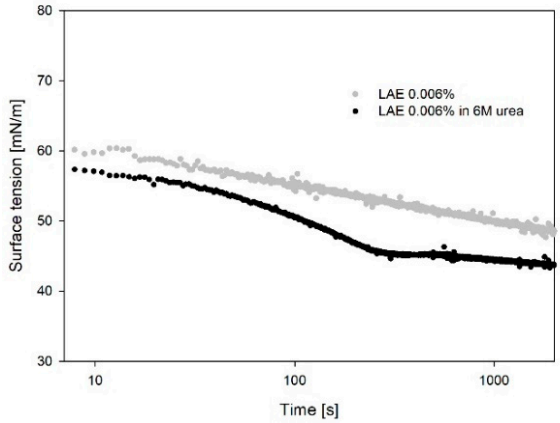

Figure 5. The effect of the addition of urea (6 mol/L) on the surface tension of 0.006 wt.% LAE—Mirenat solution (85% purity).

Sodium salicylate had the strongest effect on the surface tension, due to the surface activity of the salicylate anion that can more effectively neutralize the positive charge of LAE cations at the interface. Characteristic differences in surface tension kinetics could be observed by adding 6 M urea. The surface tension value first seemed to reach a plateau and then decreased. The addition of urea caused a faster decrease in the surface tension compared to the pure LAE-cCNC mixture; however, after the 2000 s of adsorption, similar surface tension values (c.a. 40 mN/m) could be observed. A similar effect of urea was observed for the surfactant solutions without cCNC, as demonstrated in Figure 5.

The frequency dependence of the dilational elasticity modulus measured by the oscillating drop technique was illustrated in Figure 6. For the LAE-cCNC dispersion without additives, the modulus values are similar to 0.006 wt.% LAE solution and c.a. are three times lower than LAE-sCNC at the same concentrations. That can be the effect of higher charge and bigger size of sCNC aggregates or their different arrangement at the interface. On the other hand, the imaginary part of the dilational elasticity for the surfactant solution without CNC was constant in that frequency rate and equal to 3 mN/m. Thus, the addition of 0.3 wt.% cCNC increases the dilational viscosity of an interface.

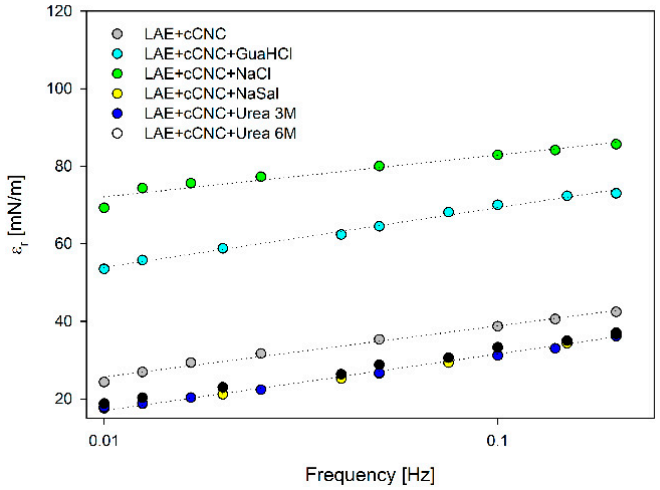

Figure 6. The frequency dependence of the dilational elasticity modulus in LAE-cCNC dispersions with the addition of 5 mmol/L electrolytes (guanidine hydrochloride, sodium chloride, sodium salicylate) and with urea at concentrations as indicated.

The addition of 5 mM NaCl resulted in the highest dilational elasticity. That can be attributed to the decrease in the electrostatic repulsion between charged cellulose nanocrystals that can pack closely at the interface. Data presented in Figure 6 indicate that adding 5 mM of guanidine hydrochloride also increased the elastic modulus (although less than 5 mmol/L NaCl); however, the surface layer became more viscous (c.f. Figure 7). The origin of that effect is unclear, but it demonstrates that both counterions and coions can affect the dilatational moduli at liquid interfaces with ionic surfactants [45]. Specific ion effects relevant for foaming were described in the literature [46]. In our case, both NaCl and GuaHCl show an almost equal effect on foaming properties of LAE-cCNC at the concentration of 5 mmol/L, despite different surface dilational viscoelastic properties. Adding 5 mmol/L NaSal or 6 mol/L urea to the LAE-cCNC dispersion caused a slight decrease in elasticity modulus compared to pure LAE-cCNC. The qualitatively different behavior of the imaginary part of the dilational modulus was observed for those dispersions. Upon addition of GauHCL, NaSal or urea, its values were increased compared to ones for LAE-cCNC, while 5 mM NaCl caused their decrease. Thus, the addition of the simple salt (NaCl) renders the interfacial layer more elastic, presumably due to closer packing of nanocrystals. The presence of hydrotropic NaSal or urea can induce forming of some dissipative structures at the interface; however, that aspect needs further investigation. In those cases, foaming was reduced: for NaSal, a relatively stable form was observed, while no stable foam could be obtained for urea.

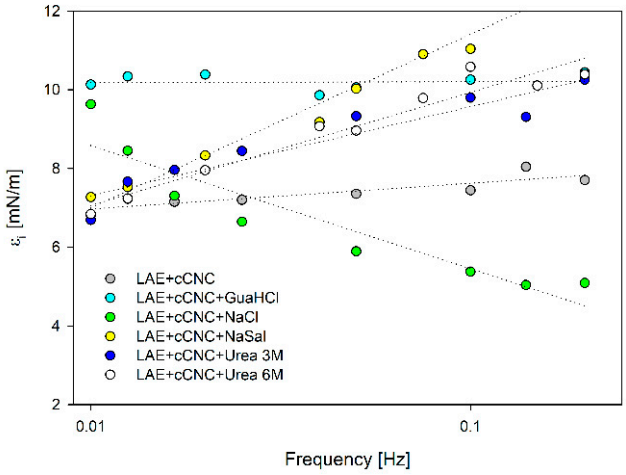

Figure 7. The frequency dependence of the imaginary part of dilational modulus in LAE-cCNC dispersions with 5 mM electrolytes: guanidine hydrochloride, sodium chloride, sodium salicylate and urea at concentrations 3 mol/L or 6 mol/L.

Our findings suggest that urea impact on the interfacial properties of LAE-cCNC dispersion can be of complex origin that is not directly reflected in the equilibrium and dynamic interfacial properties. Urea can disrupt the water structure and become oriented at the interface in the presence of ionic surfactants [37]. Due to enhanced cellulose solubility, urea can also affect the aggregation of nanocrystals and their orientation at interfaces. In particular, the stability of foams in the LAE-cCNC dispersions may be attributed to the lamellar arrangement of nanoparticles, as was demonstrated for the surfactant mesophases [47]. That arrangement may be disrupted by urea (and to a lesser extent by NaSal), which leads to foam destabilization.

4. Conclusions

Foam stability in ethyl lauroyl arginate (LAE) mixtures has a complex origin, including the adsorption of surfactant at the interface, its dynamics at the expanded/contracted interface and the formation of bulk and interfacial aggregates with carboxylated cellulose nanocrystals (cCNC), which change at the time of the foam drainage. Cellulose nanocrystals decorated with oppositely charged surfactants adsorb at the water/air interface, lower the surface tension and modify the surface viscoelastic properties. They reduce drainage and prevent coalescence. Large cellulose nanocrystals aggregates have a significant effect on foam stability, as they accumulate in the Plateau borders and prevent drainage. On the other hand, large aggregates with randomly oriented nanocrystals in the foam films can act as defoamers.

The presence of electrolytes such as sodium chloride and guanidine hydrochloride at a small concentration of 5 mM did not change foamability and foam stability, despite a two-fold increase in the surface dilational elasticity. The hydrodynamic diameter of cellulose nanocrystals also increased twice in size, due to electrostatic screening of CNC repulsion. The surface-active anion of sodium salicylate adsorbs at the interface and effectively screen electrostatic interactions of the LAE hydrophilic group. The foamability of LAE-cCNC mixtures in the presence of 5 mmol/L NaSal was much lower, but the foam stability did not change. Such an effect can be explained by the significant influence of cellulose nanocrystals on overall foam stability.

A dramatic decrease in the quantity of obtained foam volume and lack of its stability were observed for LAE-cCNC mixtures containing 6 mol/L urea. Minor changes of the equilibrium and dynamic surface tension upon the addition of urea cannot explicate that decrease. The plausible explanation can be its orientation at the interface in the presence of ionic surfactants and charged nanocrystals and the disruption of the water structure. Urea can also destroy large lamellar cCNC aggregates that reduce foam drainage. Despite the

chaotropic nature of both guanidine hydrochloride and urea, their effect on ethyl lauroyl arginate—carboxylated CNC dispersions bulk and interfacial properties—are different. The differences in the effect of those denaturants on the bulk and interfacial properties of protein solutions have been described before [48,49]. Our work is the first demonstration of the urea effect on surfactant—nanoparticles interfacial properties and foaming. Future experiments can reveal the complexity of molecular interactions in this system. Importantly, urea affects the interfacial properties of ethyl lauroyl arginate. Further experiments will reveal if it is connected to surfactant hydrolysis, formation of some interfacial structures or other effects. Detailed analysis of different urea concentrations and hydrodynamic size of cellulose nanoparticles can determine the extent of large nano-aggregates solubility. Data presenting the influence of urea on hydrodynamic size are very consistent for the LAE concentration studied. Thin film balance experiments can assess the direct influence of aggregate sizes on film stability. It should be noted that nanoparticle aggregation and their size distribution can affect the thin film stability in a complex way [50]. Investigations of thin film stability are very interesting for the explanation of the influence of some factors controlling foam stability, but other ones such as water drainage or gas permeabilities of liquid films can also be influenced by the aggregation of nanoparticles.

Author Contributions: Conceptualization, A.C. and P.W.; methodology, P.W., A.C. and M.K.; validation, A.C., P.W. and M.K.; formal analysis, P.W.; investigation, A.C.; resources, M.K.; data curation, A.C.; writing—original draft preparation, A.C.; writing—review and editing, P.W. and M.K.; visualization, A.C.; software, M.K.; supervision, P.W.; project administration, M.K.; funding acquisition, M.K. and P.W. All authors have read and agreed to the published version of the manuscript.

Funding: This research was funded by the National Science Centre of Poland (grant number 2016/21/B/ST8/02107) and statutory subsidy for Jerzy Haber Institute of Catalysis and Surface Chemistry PAS. AC has been partly supported by EU Project POWR.03.02.00-00-I004/16.

Institutional Review Board Statement: Not applicable.

Informed Consent Statement: Not applicable.

Data Availability Statement: The data presented in this study are freely available from the authors upon a reasonable request.

Acknowledgments: Figure 1b was reproduced from ref. [21] with permission from The Royal Society of Chemistry.

Conflicts of Interest: The authors declare no conflict of interest. The funders had no role in the design of the study; in the collection, analyses, or interpretation of data; in the writing of the manuscript, or in the decision to publish the results.

References

1. Klemm, D.; Kramer, F.; Moritz, S.; Lindstrom, T.; Ankerfors, M.; Gray, D.; Dorris, A. Nanocelluloses: A new family of nature-based materials. *Angew. Chem. Int. Ed.* **2011**, *50*, 5438–5466.
2. Klemm, D.; Cranston, E.D.; Fischer, D.; Gama, M.; Kedzior, S.A.; Kralisch, D.; Kramer, F.; Kondo, T.; Lindström, T.; Nietzsche, S.; et al. Nanocellulose as a natural source for groundbreaking applications in materials science: Today's state. *Materialstoday* **2018**, *21*, 720–748. [CrossRef]
3. Kontturi, E.; Laaksonen, P.; Linder, M.B.; Nonappa; Gröschel, A.H.; Orlando, J.; Rojas, O.J.; Ikkala, O. Advanced materials through assembly of nanocelluloses. *Adv. Mater.* **2018**, *30*, 1703779. [CrossRef] [PubMed]
4. Wang, J.; Carlos, C.; Zhang, Z.; Li, J.; Long, Y.; Yang, F.; Dong, Y.; Qiu, X. Piezoelectric nanocellulose thin film with large-scale vertical crystal alignment. *ACS Appl. Mater. Interfaces* **2020**, *12*, 26399–26404. [CrossRef]
5. Droguet, B.E.; Liang, H.-L.; Frka-Petesic, B.; Parker, R.M.; De Volder, M.F.L.; Baumberg, J.J.; Vignolini, S. Large-scale fabrication of structurally coloured cellulose nanocrystal films and effect pigments. *Nat. Mater.* **2021**, *21*, 352–358. [CrossRef]
6. Koshani, R.; Tavakolian, M.; van de Ven, T.G.M. Cellulose-based dispersants and flocculants. *J. Mater. Chem. B* **2020**, *8*, 10502–10526. [CrossRef]
7. Shen, X.; Shamshina, J.L.; Berton, P.; Gurau, G.; Rogers, R.D. Hydrogels based on cellulose and chitin: Fabrication, properties, and applications. *Green Chem.* **2016**, *18*, 53–75. [CrossRef]
8. Chowdhury, R.A.; Nuruddin, Md.; Clarkson, C.; Montes, F.; Howarter, J.; Youngblood, J.P. Cellulose nanocrystal (CNC) coatings with controlled anisotropy as high-performance gas barrier films. *ACS Appl. Mater. Interfaces* **2019**, *11*, 1376–1383. [CrossRef]

9. Gicquel, E.; Bras, J.; Rey, C.; Putaux, J.-L.; Pignon, F.; Jean, B.; Martin, C. Impact of sonication on the rheological and colloidal properties of highly concentrated cellulose nanocrystal suspensions. *Cellulose* **2019**, *26*, 7619–7634. [CrossRef]
10. Chakraborty, A.; Nonappa; Mondal, B.; Chaudhari, K.; Rekola, H.; Hynninen, V.; Kostiainen, M.A.; Ras, R.H.A.; Pradeep, T.J. Near-infrared chiral plasmonic microwires through precision assembly of gold nanorods on soft biotemplates. *Phys. Chem. C* **2021**, *125*, 3256–3267. [CrossRef]
11. Lavoine, N.; Bergström, L. Nanocellulose-based foams and aerogels: Processing, properties, and applications. *J. Mater. Chem. A* **2017**, *5*, 16105–16117. [CrossRef]
12. Lam, S.; Velikov, L.P.; Velev, O.D. Pickering stabilization of foams and emulsions with particles of biological origin. *Curr. Opin. Colloid Interface Sci.* **2014**, *19*, 490–500. [CrossRef]
13. Vanderfleet, O.M.; Cranston, E.D. Production routes to tailor the performance of cellulose nanocrystals. *Nat. Rev. Mater.* **2021**, *6*, 124–144. [CrossRef]
14. Andrews, M.P.; Morse, T. Method for Producing Functionalized Nanocrystalline Cellulose and Functionalized Nanocrystalline Cellulose Thereby Produced. U.S. Patent 20,170,260,298 A1, 14 September 2017.
15. Usov, I.; Nyström, G.; Adamcik, J.; Handschin, S.; Schütz, C.; Fall, A.; Bergström, L.; Mezzenga, R. Understanding nanocellulose chirality and structure–properties relationship at the single fibril level. *Nat. Commun.* **2015**, *6*, 7564. [CrossRef]
16. Surov, O.V.; Voronova, M.I.; Zakharov, A.G. Functional materials based on nanocrystalline cellulose. *Russ. Chem. Rev.* **2017**, *86*, 907–933. [CrossRef]
17. Kang, K.; Eremin, A. Solvent-dependent morphology and anisotropic microscopic dynamics of cellulose nanocrystals under electric fields. *Phys. Rev. E* **2021**, *103*, 032606. [CrossRef] [PubMed]
18. Czakaj, A.; Jarek, E.; Krzan, M.; Warszyński, P. Ethyl lauroyl arginate, an inherently multicomponent surfactant system. *Molecules* **2021**, *26*, 5894. [CrossRef]
19. Drenckhan, W.; Saint-Jalmes, A. The science of foaming. *Adv. Colloid Interface Sci.* **2015**, *222*, 228–259. [CrossRef]
20. Briceño-Ahumada, Z.; Drenckhan, W.; Langevin, D. Coalescence in draining foams made of very small bubbles. *Phys. Rev. Lett.* **2016**, *116*, 128302-1-5. [CrossRef]
21. Czakaj, A.; Kannan, A.; Wiśniewska, A.; Grześ, G.; Krzan, M.; Warszyński, P.; Fuller, G.G. Viscoelastic interfaces comprising of cellulose nanocrystals and lauroyl ethyl arginate for enhanced foam stability. *Soft Matter* **2020**, *16*, 3981–3990. [CrossRef]
22. Kalashnikova, I.; Bizot, H.; Bertoncini, P.; Cathalaa, B.; Capron, I. Cellulosic nanorods of various aspect ratios for oil in water Pickering emulsions. *Soft Matter* **2013**, *9*, 952–959. [CrossRef]
23. Kalashnikova, I.; Bizot, H.; Cathala, B.; Capron, I. Modulation of cellulose nanocrystals amphiphilic properties to stabilize oil/water interface. *Biomacromolecules* **2012**, *13*, 267–275. [CrossRef] [PubMed]
24. Cervin, N.T.; Johansson, E.; Benjamins, J.-W.; Wågberg, L. Mechanisms behind the stabilizing action of cellulose nanofibrils in wet-stable cellulose foams. *Biomacromolecules* **2015**, *16*, 3, 822–831. [CrossRef] [PubMed]
25. Fazilati, M.; Ingelsten, S.; Wojno, S.; Nypelö, T.; Kádár, R. Thixotropy of cellulose nanocrystal suspensions. *J. Rheol.* **2021**, *65*, 1035. [CrossRef]
26. Bertsch, P.; Diener, M.; Adamcik, J.; Scheuble, N.; Geue, T.; Mezzenga, R.; Fischer, P. Adsorption and interfacial layer structure of unmodified nanocrystalline cellulose at air/water interfaces. *Langmuir* **2018**, *34*, 15195–15202. [CrossRef]
27. Delepierre, G.; Eyley, S.; Thielemans, W.; Weder, C.; Cranston, E.D.; Zoppe, J.O. Patience is a virtue: Self-assembly and physicochemical properties of cellulose nanocrystal allomorphs. *Nanoscale* **2020**, *12*, 17480–17493. [CrossRef]
28. Hu, Z.; Xu, R.; Cranston, E.D.; Pelton, R.H. Stable aqueous foams from cellulose nanocrystals and methyl cellulose. *Biomacromolecules* **2016**, *17*, 4095–4099. [CrossRef]
29. Xiang, W.; Preisig, N.; Ketola, A.; Tardy, B.L.; Bai, L.; Ketoja, J.A.; Stubenrauch, C.; Rojas, O.J. Surface activity and foaming capacity of aggregates formed between an anionic surfactant and non-cellulosics leached from wood fibers. *Biomacromolecules* **2019**, *20*, 6, 2286–2294. [CrossRef]
30. Para, G.; Jarek, E.; Warszyński, P.; Adamczyk, Z. Effect of electrolytes on surface tension of ionic surfactant solutions. *Colloids Surf. A Physicochem. Eng. Asp.* **2003**, *222*, 213–222. [CrossRef]
31. Sharma, V.K.; Srinivasan, H.; Mitra, S.; Garcia-Sakai, V.; Mukhopadhyay, R.J. Effects of hydrotropic salt on the nanoscopic dynamics of DTAB micelles. *Phys. Chem. B* **2017**, *121*, 5562–5572. [CrossRef]
32. Ogawa, T.; Matsumura, Y. Revealing 3D structure of gluten in wheat dough by optical clearing imaging. *Nat. Commun.* **2021**, *12*, 1708. [CrossRef] [PubMed]
33. Tschoegl, N.W.; Alexander, A.E. The surface chemistry of wheat gluten II. Measurements of surface viscoelasticity. *J. Colloid Sci.* **1960**, *15*, 168–182. [CrossRef]
34. Ruiz, C.C. Micelle formation and microenvironmental properties of sodium dodecyl sulfate in aqueous urea solutions. *Colloids Surf. A Physicochem. Eng. Asp.* **1999**, *147*, 349–357. [CrossRef]
35. Kumari, S.; Sonu, K.; Halder, S.; Aggrawal, R.; Sundar, G.; Saha, S.K. Effect of urea on solvation dynamics and rotational relaxation of coumarin 480 in aqueous micelles of cationic gemini surfactants with different spacer groups. *ACS Omega* **2018**, *3*, 3079–3095. [CrossRef]
36. Kancharla, S.; Dong, D.; Bedrov, D.; Tsianou, M.; Alexandridis, P. Structure and interactions in perfluorooctanoate micellar solutions revealed by small-angle neutron scattering and molecular dynamics simulations studies: Effect of urea. *Langmuir* **2021**, *37*, 17, 5339–5347. [CrossRef]

37. Moll, C.J.; Versluis, J.; Bakker, H.B. Direct observation of the orientation of urea molecules at charged interfaces. *J. Phys. Chem. Lett.* **2021**, *12*, 10823–10828. [CrossRef]
38. Xiong, B.; Zhao, P.; Hu, K.; Zhang, L.; Cheng, G. Dissolution of cellulose in aqueous NaOH/urea solution: Role of urea. *Cellulose* **2014**, *21*, 1183–1192. [CrossRef]
39. Heyda, J.; Okur, H.I.; Hladilkova, J.; Rembert, K.B.; Hunn, W.; Yang, T.; Dzubiella, J. Guanidinium can both cause and prevent the hydrophobic collapse of biomacromolecules. *J. Am. Chem. Soc.* **2017**, *139*, 863–870. [CrossRef]
40. Delepierre, G.; Vanderfleet, O.M.; Niinivaara, E.; Zakani, B.; Cranston, E.D. Benchmarking cellulose nanocrystals Part II: New industrially produced materials. *Langmuir* **2021**, *37*, 8393–8409. [CrossRef]
41. Bhattacharjee, S.J. In relation to the following article "DLS and zeta potential—What they are and what they are not?". *Control. Release* **2016**, *235*, 337–351. [CrossRef]
42. Javadi, A.; Mucic, N.; Karbaschi, M.; Won, J.Y.; Fainerman, V.B.; Sharipova, A.; Aksenenko, E.V.; Kovalchuk, V.I.; Kovalchuk, N.M.; Makievski, A.; et al. Interfacial Dynamics Methods. In *Encyclopedia of Colloid and Interface Science*; Tadros, T., Ed.; Springer: Berlin/Heidelberg, Germany, 2013.
43. Loglio, G.; Pandolfini, P.; Miller, R.; Makievski, A.V.; Ravera, F.; Ferrari, M.; Liggieri, L. Drop and bubble shape analysis as tool for dilational rheology studies of interfacial layers. In *Novel Methods to Study Interfacial Layers*; Möbius, D., Miller, R., Eds.; Elsevier: Amsterdam, The Netherlands, 2001; pp. 439–483.
44. Ravera, F.; Ferrari, M.; Santini, E.; Liggieri, L. Influence of surface processes on the dilational visco-elasticity of surfactant solutions. *Adv. Colloid Interface Sci.* **2005**, *117*, 75–100. [CrossRef] [PubMed]
45. Firouzi, M.; Kovalchuk, V.I.; Loglio, G.; Miller, R. Salt effects on the dilational viscoelasticity of surfactant adsorption layers. *Curr. Opin. Colloid Interface Sci.* **2022**, *57*, 101538. [CrossRef]
46. Amani, P.; Karakashev, S.I.; Grozev, N.A.; Simeonova, S.S.; Miller, R.; Rudolph, V.; Firouzi, M. Effect of selected monovalent salts on surfactant stabilized foams. *Adv. Colloid Interface Sci.* **2021**, *295*, 102490. [CrossRef] [PubMed]
47. Briceño-Ahumada, Z.; Maldonado, A.; Impéror-Clerc, M.; Langevin, D. On the stability of foams made with surfactant bilayer phases. *Soft Matter* **2016**, *12*, 1459–1467. [CrossRef]
48. Lim, W.K.; Rösgen, J.; Englander, S.W. Urea, but not guanidinium, destabilizes proteins by forming hydrogen bonds to the peptide group. *Proc. Natl. Acad. Sci. USA* **2009**, *106*, 2595–2600. [CrossRef]
49. Tikhonov, M.M.; Akentiev, A.V.; Noskov, B.A. Influence of guanidine hydrochloride and urea on the dynamic surface properties of lysozyme solutions. *Mendeleev Commun.* **2015**, *25*, 288–289. [CrossRef]
50. Rullier, B.; Axelos, M.A.V.; Langevin, D.; Novales, B. β-Lactoglobulin aggregates in foam films: Effect of the concentration and size of the protein aggregate. *J. Colloid Interface Sci.* **2010**, *343*, 330–337. [CrossRef]